Iterative Rekonstruktion

Vorlesung FH-Hagenberg
SE:MED

Principles of Emission Tomography

- Biological processes are visualized using radioactive tracers
- Quasi-stationary accumulation of tracer is employed for diagnostic routines (tumour staging, stroke, heart diseases)
- spatial detecton of γ-quanta associated the location of the emission to a line of response (collimator-SPECT, coincidence measurement -PET)
- Transversal slices are reconstructed from projection data
- Stacked slices form an image volume

Radon Transform - Projection Geometry

Projection or data acquisition. Information about the object is integrated along the line L and transformed into a point-information according to its co-ordinates *l* and Θ.

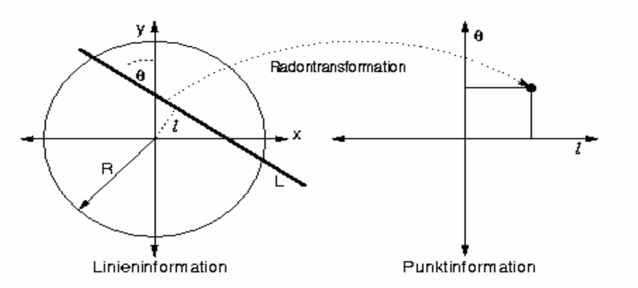

Medizinische Bildverarbeitung Werner Backfrieder

3D Projection Data - Sinograms

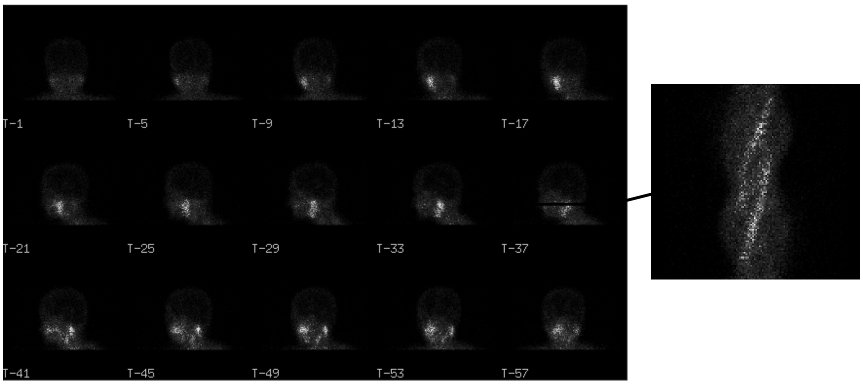

Medizinische Bildverarbeitung Werner Backfrieder

Iterative Reconstruction: Problem Statement

- Image volume and all projection data form the image vector ***X*** and the measurement vector ***Y***.
- System of Equations

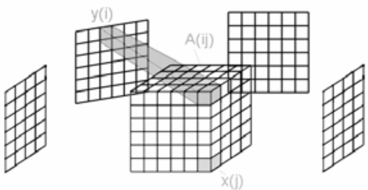

Iterative Reconstruction: System Matrix

- The elements a_{ij} of the system matrix *A* give the probability of the detection-event in bin y_i of a g-quantum emitted from voxel x_j.
- The following system properties are modelled by matrix *A*
  - scanner geometry
  - scatter
  - attenuation
  - detector efficiacy
- Y=AX has no exact solution
  - noise -> inconsitent system of equations
  - number of equations ≠ number of unknowns
- **Feasible solution by iterative algorithm**

Iterative Reconstruction: Algorithm

1. Starting image $\mathbf{X}_0$
2. Pseudo projection $\mathbf{Y'}=\mathbf{AX}_0$
3. Comparison of measured data $\mathbf{Y}$ with pseudo projection data $\mathbf{Y'}$
4. Update of Image data $\mathbf{X}_n \rightarrow \mathbf{X}_{n+1}$
5. $\mathbf{X}_n$ and $\mathbf{X}_{n+1}$ meet stopping criterium
   1. $\mathbf{X}_{n+1}$ is feasible solution
6. else
   1. continue with step 2

Arithmetic Reconstruction Technique (ART)

Additive ART

$$x_j^{(n+1)} = x_j^{(n)} + \frac{y_i - \sum_l a_{ij'} x_{j'}^{(n)}}{\sum_{j'} a_{ij'}} a_{ij}$$

Multiplicative ART

$$x_j^{(n+1)} = x_j^{(n)} * \frac{y_i}{\sum_{j'} a_{ij'} x_{j'}^{(n)}}$$

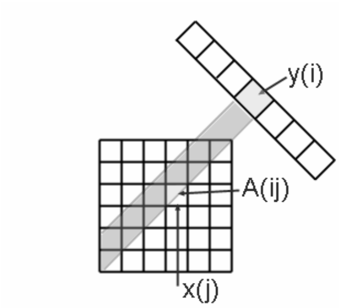

Medizinische Bildverarbeitung Werner Backfrieder

Convergence of additive ART

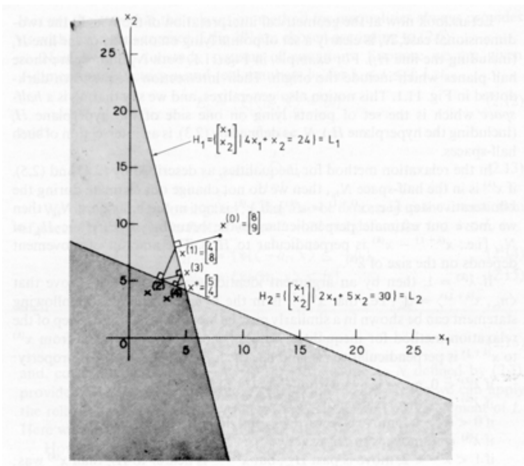

Simple example (2 pixel and 2 projection values) for the illustration of the convergence of additive ART.

Statistical Models: ML-EM

Poisson distribution: $p_\lambda(y) = \frac{\exp(-\lambda) * \lambda^y}{y!}$

Expectation value : $\lambda_i = \sum_j a_{ij} x_j$

Measurement value: y_i

Log-Likelihood: $p(y \mid x) = \sum_i (y_i \log(\sum_j a_{ij} x_j) - \sum_j a_{ij} x_j)$

Iteration step:

$$x_j^{(n+1)} = x_j^{(n)} * \frac{\sum_i a_{ij} \frac{y_i}{\sum_{j'} a_{ij'} x_{j'}^{(n)}}}{\sum_i a_{ij}}$$

ML-EM

$$x_j^{(n+1)} = x_j^{(n)} * \frac{\sum_i a_{ij} \frac{y_i}{\sum_{j'} a_{ij'} x_{j'}^{(n)}}}{\sum_i a_{ij}}$$

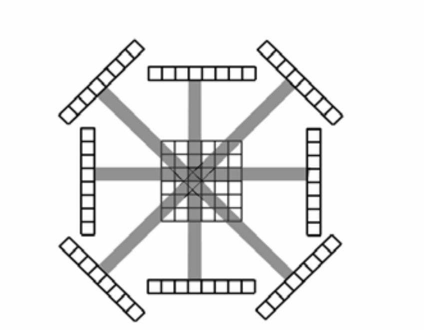

Convergence of ML-EM

ML-EM is a maximum entropy approach, towards high iterations noise deteriorates the image.

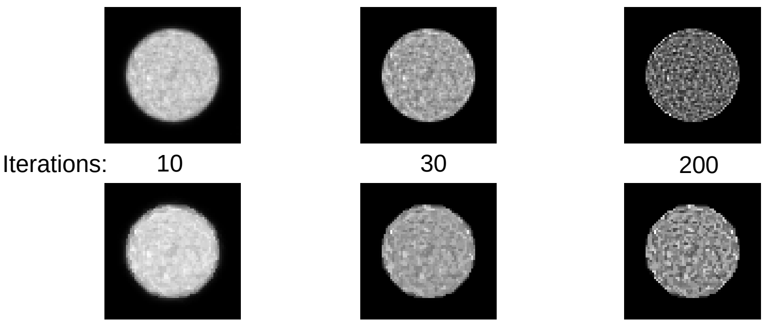

Prior information is implemented to provide inherent smoothing during reconstruction.

Bayesian Methods: Penalty Terms

MAP-density

$$p(X|Y) \propto p(Y|X) * p(x)$$

Penalty term

$$P(X) = e^{-\alpha E(X)}$$

Median root prior

$$E(X) = \frac{(X-M)^2}{2M}$$

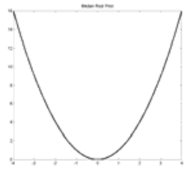

One step late algorithm

OSL

$$x_l^{(n+1)} = x_l^{(n)} \frac{\sum_k a_{kl} \frac{y_k}{\sum_m a_{km} x_m^{(n)}}}{\sum_k a_{kl} - \left.\frac{\partial \ln P(X)}{\partial x_l}\right|_{x_l = x_l^{(n)}}}$$

Acceleration: Ordered Subsets

- A series of subsets {S} of the measurement values Y is defined
- ML-EM algorithm is calculated with each subset {S} until stopping criterion is fulfilled
- Convergence is accelerated

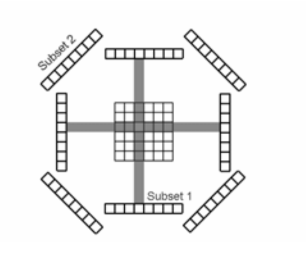

$$x_j^{(n+1)} = x_j^{(n)} * \frac{\sum_{i \in \{S\}} a_{ij} \frac{y_i}{\sum_{j'} a_{ij'} x_{j'}^{(n)}}}{\sum_i a_{ij}}$$

Attenuation Correction

PET

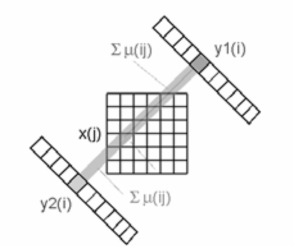

$$y_{ij} \propto a_{ij} x_j \exp(-\int_0^x \mu(L)dL) * a_{ij} x_j \exp(-\int_x^{L_{end}} \mu(L)dL) =$$

$$= a_{ij} x_j \exp(-\int_0^{L_{end}} \mu(L)dL)$$

SPECT

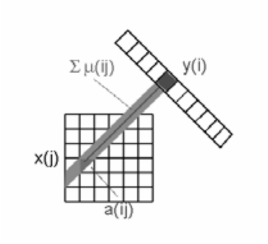

$$y_{ij} \propto a_{ij} x_j \exp(-\int_0^x \mu(L)dL)$$

$$y_{ij} \propto a_{ij} x_j \exp(\sum_{k \in L} \mu_{ik})$$

Mathematical phantom

Mathematical phantom consisting of elliptical structures for simulating both distribution of radio-tracer and non-uniform attenuation:

- **elliptical background (big ellipsis)**
- **two elliptical hot spots**
- **uniform attenuation in big ellipsis**
- **high attenuation in circular area between hot spots (colon)**
- **Poisson distributed noise in simulated projection values**

Mathematical phantom

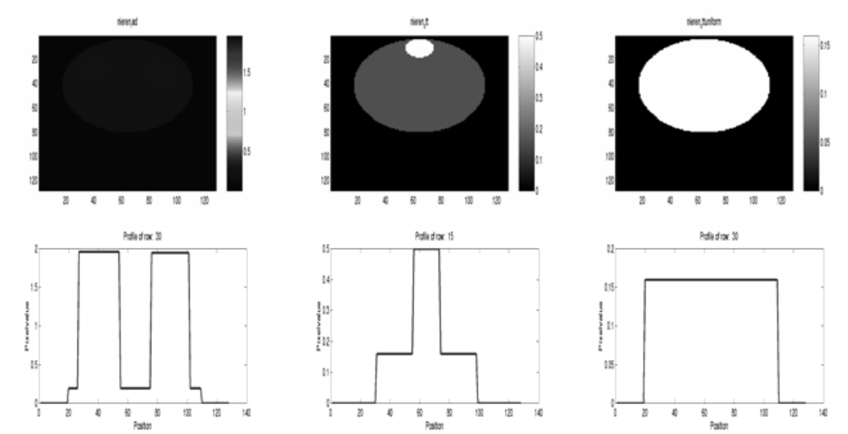

Distribution of radio-active tracer.

Attenuation coefficients used in simulation and non-uniform attenuation correction

Attenuation coefficients used for uniform correction.

Mathematical phantom: results 1

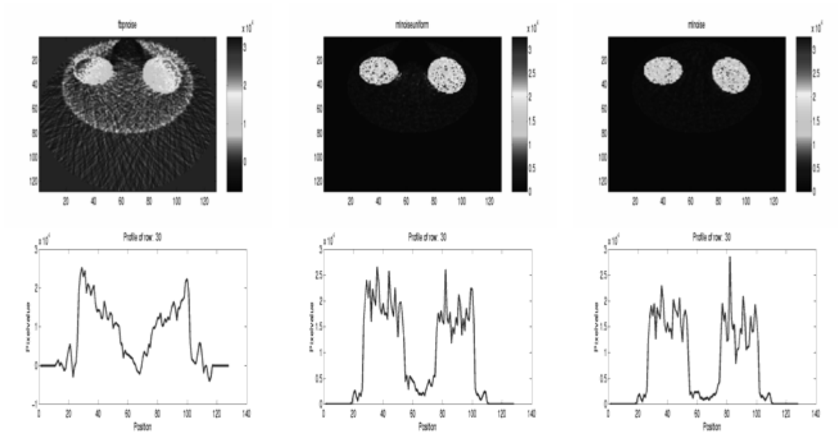

FBP, α=0.8

ML-EM, uniform, 50it

ML-EM,non-uniform, 50it

Mathematical phantom: median root prior, 50 iterations

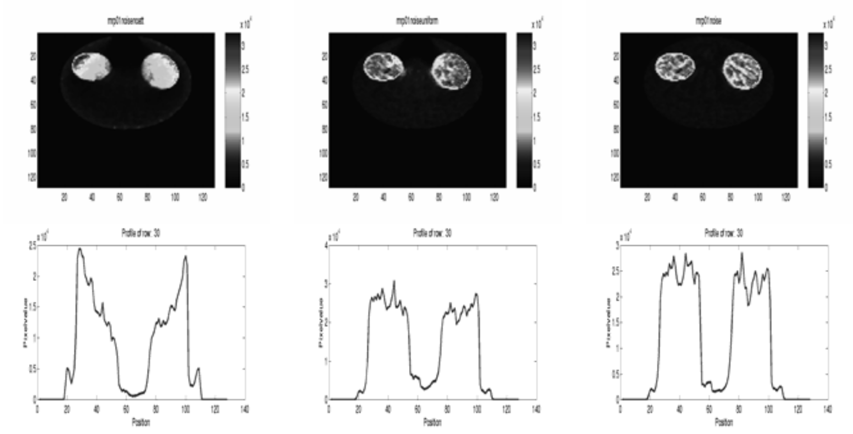

No correction | Uniform correction | Non-uniform correction

Jaszczak phantom: 2GBq 99mTc, Picker Prism3000, FOV=46cm, 128x128 Matrix, 3.6mm slice thickness, 3° and 60s/step

ML-EM, 50it., no attenuation correction

ML-EM, 50it., non-uniform attenuation correction

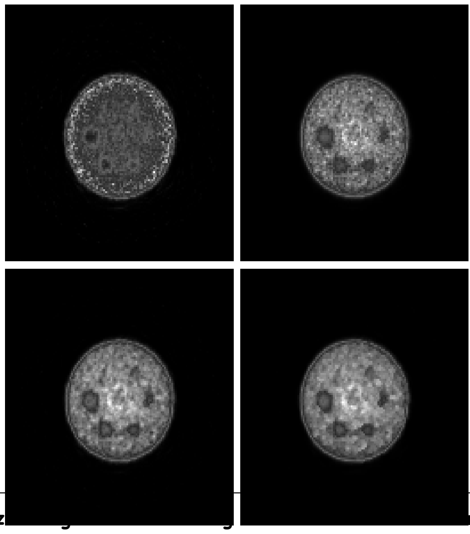

MAP-Gibbs' prior, α=2, β=0.01, 50it., non-uniform attenuation correction

MRP, α=0.1, 50it., non-uniform attenuation correction

Alderson phantom

- kidneys 50 MBq 99mTc, each
- bladder 150 MBq 99mTc
- body-background 80 MBq 99mTc
- colon Teflon cylinder 23mm diameter

Picker PRISM3000, 3°/step, 20s/step, circular orbit, 46cm FOV,3.6mm slice thickness, 128x128 matrix

Philps Tomoscan SR7000, 120kV, 200mA, 34.8cm FOV, 5mm slice thickness, 512x512 matrix, planar-mode

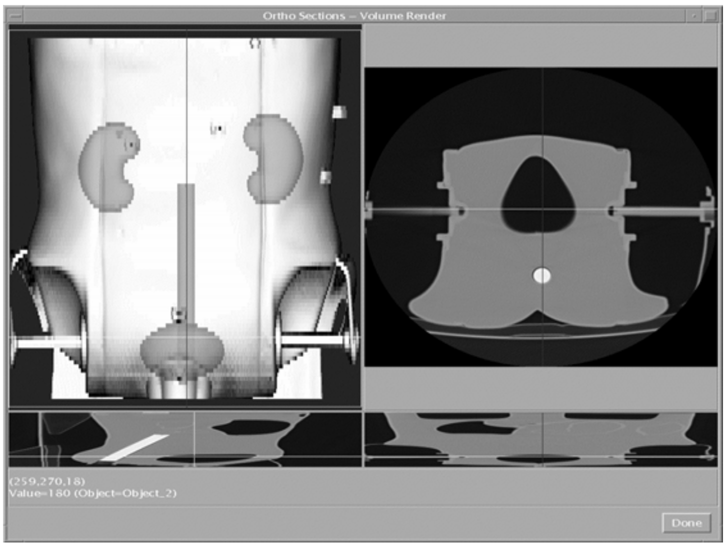

3D rendering and orthogonal sections of the Alderson phantom. Kidneys, bladder and colon are segmented.

Alderson phantom: results1

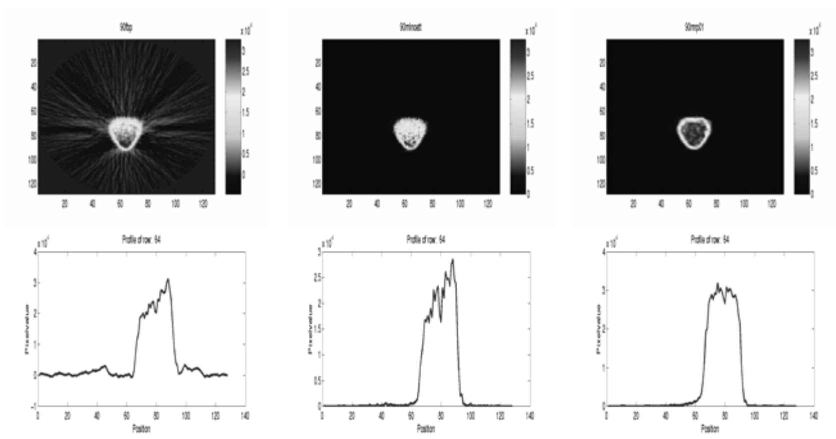

FBP, α=0.8 | ML-EM, no correction | MRP, non-uniform correction

Alderson phantom: ordered subsets (OS)

MAP-Gibbs' prior, α=2, β=0.01, 50it., non-uniform attenuation correction

MRP, α=0.1, 50it., non-uniform attenuation correction

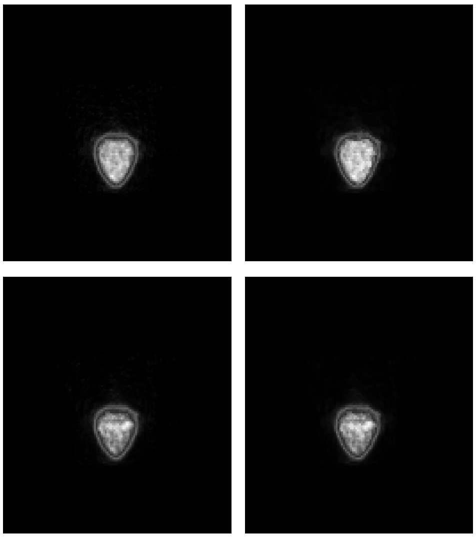

MAP-Gibbs' prior, 15 subsets, 3 it. / subset

MRP, 15 subsets, 3it. / subset

In-vivo data from head and neck area

CT and SPECT data from the head and neck area:
SPECT: Prism3000, 99mTc Sestamibi, 128x128, FOV 46cm, 3o, 20s
CT: Tomoscan SR7000, 120kV, 400mA, 512x512, FOV 185mm

Segmentation of 3 components:
bone 0.295/cm soft-tissue: 0.1596/cm air:0/cm

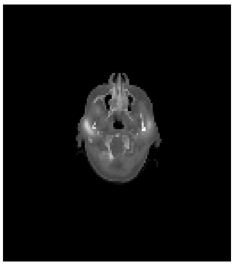

Overlay of CT and SPECT image data

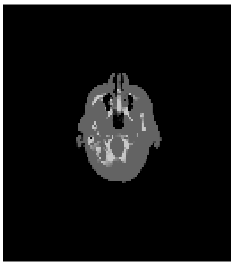

Reformatted and segmented CT image

Results: in-vivo data

MAP-Gibbs' prior, $\alpha=2$, $\beta=0.025$, 50it., no attenuation correction

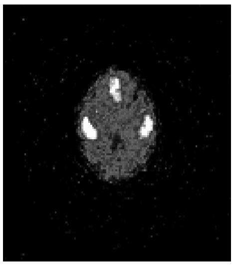

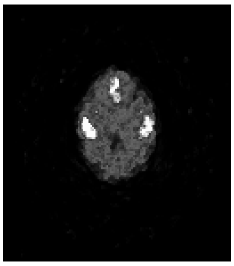

MRP, $\alpha=0.1$, 50it., no attenuation correction

MAP-Gibbs' prior, $\alpha=2$, $\beta=0.025$, 50it., non-uniform attenuation correction

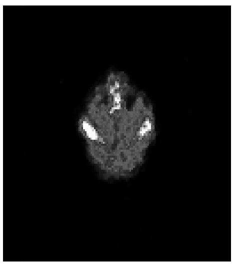

MRP, $\alpha=0.1$, 50it., non-uniform attenuation correction

Scatter: a problem in 3D

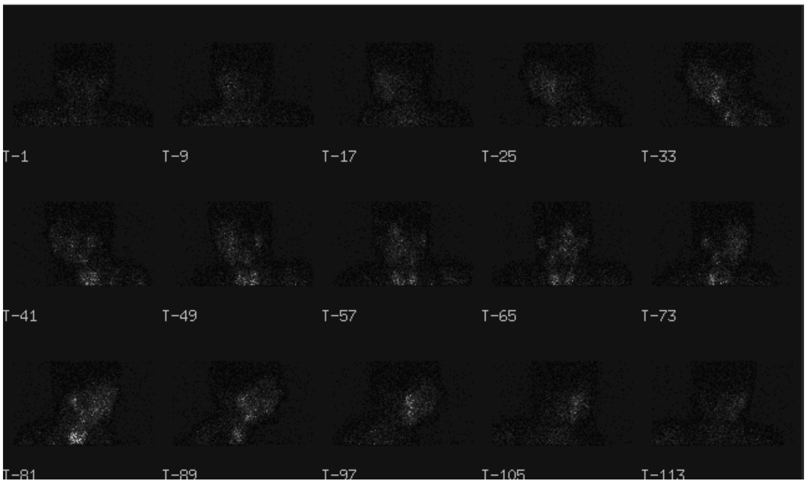

Parallel Computing Concepts

- Single task computing systems (MS-DOS)
- Multitasking OS (Unix, NT)
- Multitasking OS with multiple CPU's
- Threads on multitasking systems
- Sending messages on multitasking OS

Concepts of Parallel Computing

- SMP: symmetric multiprocessing
  - multiple processors use shared memory
  - bus based communication
  - distributed shared memory

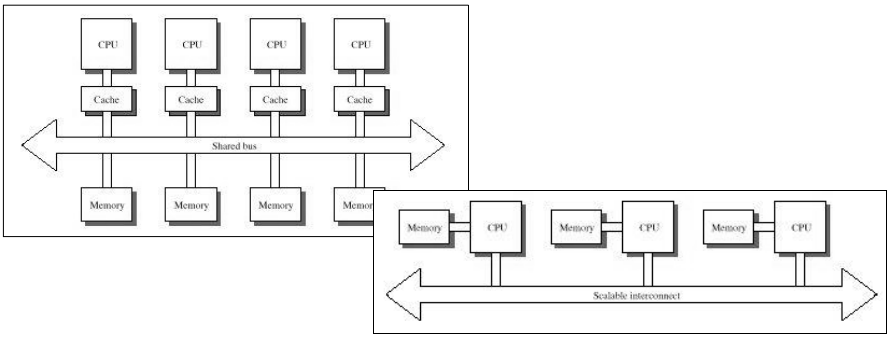

Concepts of Parallel Computing

- Distributed memory machines.
  - Each node has ist own memory.
  - Communication via message passing
  - connected by fast Ethernet.
  - Beowulf - Linux Cluster

    zB. Avalon Cluster at Los Alamos 70 Alpha Workstations (533 MHz CPUs) 73 Gflops 150.000$

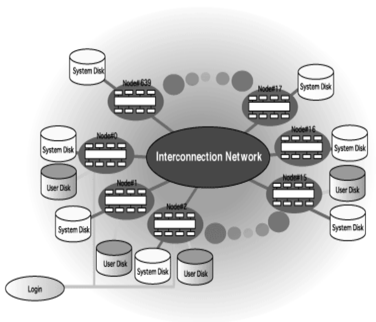

Earth Simulator (NEC)